

Mercury dynamics and mass balance in a subtropical forest, southwestern China

Ma Ming^a, Wang Dingyong^{a,b,*}, Du Hongxia^a, Sun Tao^a, Zhao Zheng^a, Wang Yongmin^a, Wei Shiqiang^a

^a College of Resources and Environment, Southwest University, Chongqing 400715, China

^b Chongqing Key Laboratory of Agricultural Resources and Environment, Chongqing 400715, China

Abstract: The mid-subtropical forest area in southwest China was affected by anthropogenic mercury (Hg) emissions over the past three decades. We quantified mercury dynamics on the forest field and measured fluxes and pools of Hg in litterfall, throughfall, stream water and forest soil in an evergreen broad-leaf forest field in southwestern China. Total Hg (THg) input by the throughfall and litterfall were assessed at 32.2 and 42.9 $\mu\text{g m}^{-2} \text{yr}^{-1}$, respectively, which were remarkably higher than those observed from other forest fields in the background of North America and Europe. Hg fluxes across the soil/air interface (18.6 $\text{mg m}^{-2} \text{yr}^{-1}$) and runoff/stream flow (7.2 $\mu\text{g m}^{-2} \text{yr}^{-1}$) were regarded as the dominant ways for THg export from the forest field. The forest field hosts an enormous amount of atmospheric Hg, and its reserves is estimated to 25341 $\mu\text{g m}^2$. The ratio of output to input Hg fluxes (0.34) is higher comparing with other study sites. The higher output/input ratio may represent an important ecological risk for the downstream aquatic ecosystems, even if the forest field could be an effective sink of Hg.

Keywords: Mercury; flux; output/input ratio; deposition; subtropical forest

***Corresponding author: Wang Dingyong**

Telephone: +86 23 68251691

Fax: +86 23 68250444

E-mail address: dywang@swu.edu.cn

Mailing address: College of Resources and Environment, Southwest University, No. 2, Tiansheng Road, Beibei District, Chongqing, P. R. China

Postcode: 400715

1. Introduction

Mercury (Hg) can cause damage to the environment and human health due to its extreme toxicity. It is well established that gaseous Hg can travel a long distance in the atmosphere so that aquatic systems in remote regions can be impacted by Hg pollution through deposition from the atmosphere (Lindberg et al., 2002a, b; Feng et al., 2009a, b). As a consequence, atmospheric deposition is the principal form of total Hg (THg) input to aquatic systems in remote pristine regions. Although Hg emissions must be reduced to mitigate current Hg contamination in surface water and fish, the magnitude of that reduction is a critical policy debate.

Forest ecosystem is generally regarded as an active pool of Hg. Hg transformation processes in the forest is considered as a vital part of global Hg cycling (Ericksen et al., 2003; Sigler et al., 2009). Most of the Hg accumulated in canopy foliage comes from atmospheric sources, rather than root uptake (Ericksen et al., 2003; Stamenkovic and Gustin, 2009). The forest canopy is a major receptor of Hg in forested landscapes (St. Louis et al., 2001). The deposited Hg to the forest may produce a certain ecological risk on the biogeochemical cycle of Hg in the forest watersheds. Hg accumulated in the forest soil may be considered as a source of both total and methyl Hg (MeHg) to aquatic ecosystems through runoff/stream flow. Moreover, Hg in the forest soil and decomposed litterfall can transfer into MeHg, resulting in increased MeHg levels in downstream

45 wet areas. Thus the release of Hg compounds from the forest field can be considered as an initial
46 step of Hg mobilization in forested catchments, and seems to be of high importance for its
47 mobility.

48

49 Biogeochemical mass balance studies quantifying Hg pools and fluxes in the forest ecosystem are
50 essential for assessing current rates of Hg inputs to, retention within, and release from terrestrial
51 ecosystems. Major research initiatives have improved our understanding of current Hg pools and
52 fluxes (Grigal et al., 2000; Schwesig and Matzner, 2001), however, knowledge of the internal
53 cycling dynamics controlling retention within and release from these ecosystems which are
54 located in the elevated Hg emitting regions is still limited (Demers et al., 2007). China's rapid
55 economic development is predicted to increase the emission of atmospheric Hg (Fu et al., 2008a,
56 b). The coal burning leads to Hg pollution in industrial and urban areas, as well as remote areas
57 due to the long-range atmospheric transport of Hg (Feng and Qiu., 2008; Fu et al., 2009). In
58 this study, we conducted a full-scale investigation on the distribution of Hg in the throughfall,
59 litterfall and precipitation for a year. At the same time, we calculated the output and input of Hg
60 during the study period. Thus, the objectives of this study were to: 1) evaluate the deposition and
61 output fluxes of Hg in the forest field and the accumulation of THg in a subtropical forest soil pool
62 of southwest China, 2) discuss Hg import and export characteristics via deposition and
63 runoff/stream flow in the study field, and 3) explore the main factors affecting Hg deposition,
64 retention within and output fluxes in the subtropical forest ecosystem.

65 **2 Materials and methods**

66 **2.1 Site description**

67 We conducted this research at Mt. Simian National Natural Reserve (106° 22' ~106° 25' E, 28°
68 35'~28° 39' N), which is situated about 200 km away from Chongqing city (Fig. 1). Chongqing is
69 the largest industrial city in southwest China, where combustion of coal accounted for more than
70 75% of the regional energy supplies in recent years. The study area has a subtropical monsoon
71 climate, with abundant rainfall every year. The mean annual temperature is 13.7 °C, with the
72 highest and lowest records in August (average: 31.5 °C) and January (averages: -5.5 °C)
73 respectively. The mean annual precipitation in the study area is 1,522.3 mm with a daily
74 maximum up to 160.5 mm (Lv et al, 2014). There are four seasons in Chongqing, spring (March
75 to May), summer (June to August), autumn (September to November), and winter (December to
76 February), with a well-defined wet/warm season from June to October. The study area is typical of
77 the region with hills of 1394 m and watersheds of about 100.1 km². The evergreen broad-leaf
78 forest selected in our research is believed to be one of the most representative vegetation types
79 preserved in the study reserve due to the following reasons. First, it is one of the most complete
80 forest located in the place between Chongqing and Guizhou. Second, it is almost all subtropical
81 forest and until recent decades is one of Asia's least populated and most inaccessible areas. Third,
82 it is the only largest and intact forest in the same latitude of the earth. Therefore, the evergreen
83 broad-leaf forest was selected as the representative forest of subtropical vegetation in this
84 research.

85 **2.2 Sampling methods and analysis**

86 **2.2.1 Sampling method of throughfall and precipitation**

87 The throughfall samples were obtained from the evergreen broad-leaf forest where Hg dynamics
88 have been investigated for one year, from March 2012 to February 2013. The precipitation

89 samples were collected by automatic precipitation samplers (APS-3A, Changsha Xianglan
90 Scientific Instruments Co., Hunan, China), which were placed on the forest field of the sampling
91 site. The throughfall was collected and measured using the same rain gauges (APS-3A, Ma et al.,
92 2015). Four rain gauges were randomly placed in each of the three 20×20 m² permanent
93 observation plots in each plantation, resulting in 12 throughfall sampling points for each plantation.
94 The containers were pre-washed with dilute (5%) HCl and thoroughly rinsed with deionized water
95 after each sampling. Moreover, the throughfall and precipitation samples were collected after each
96 precipitation event from each site during the sampling period.

97 The volume-weighted mean concentration (VWM) is obtained with the formula introduced in
98 Acid Deposition Monitoring Network in East Asia, 2012:

$$99 \quad \text{VWM} = (X_1 \times V_1 + X_2 \times V_2 + \dots + X_t \times V_t) / (V_1 + V_2 + \dots + V_t) = \sum (X_t \times V_t) / \sum V_t$$

100 where, X_t means the ion concentration in each precipitation event (ng L⁻¹), V_t means the volume of
101 each rainfall (mm).

102 Hg flux was determined by multiplying Hg concentrations by the volume of precipitation
103 collected. Wet deposition fluxes of THg and MeHg were calculated according to the following
104 equation:

$$105 \quad F_w = \frac{1}{1000} \sum_{i=1}^{i=n} (C_R^i p^i)$$

106 where, F_w is the annual THg or MeHg wet deposition flux (mg m⁻² yr⁻¹), C_i is the VWM (ng L⁻¹) of
107 each rain sample, and P_i (mm) is the precipitation or throughfall amount.

108 **2.2.2 Sampling method of the stream**

109 The stream/runoff was collected at the edge of the forest catchment. For the water yield of the
110 stream/runoff, it was monitored in the outlets of the forest catchment by the local hydrological
111 departments. Stream water samples for analysis were collected in 7 sampling sites every two
112 weeks from March 2012 to February 2013. The 250 ml Teflon bottles were used to collect the
113 stream water samples. All Teflon bottles were cleaned with detergent, thoroughly rinsed with tap
114 water, boiled in a 30% HNO₃ solution (v/v) for 1.5 h, rinsed and filled with Milli-Q water.
115 Trace-metal grade HCl was immediately treated to the samples to acidify them. It should be noted
116 that the water samples were not filtered and thus represented the stream load of THg. The
117 subtropical forest field in the study area is 100.1 km². Annual water discharge of the study site is
118 1.86×10⁸ m³ (hydrological departments of Jiangjin district). The annual precipitation (Table 1) of
119 the sampling site is slightly lower than the annual discharge. Therefore, it can be assumed that the
120 calculation has certain representativeness. Volume weighted concentrations were computed by the
121 stream/runoff collected during the study period. The fluxes were achieved by multiplying the
122 average Hg concentration by the total amount of runoff during the study period.

123 **2.2.3 Sampling method of litterfall and soil pool**

124 The litter samples were collected by self-made litter collectors (0.5 m×0.5 m), which were made
125 from treated lumber with a screen bottom. During the study period, the collectors were placed at
126 four different sites within the study field. The litter collected was saved in brown paper bags and
127 transported to the laboratory under 4°C, and then air-dried in clean environment in the laboratory
128 until analysis. Soil samples were collected at five different sites in each field using polyvinyl
129 chloride pipes (2.54 cm). Soil samples were obtained from 5 soil profiles. Three layers (O_i , O_e ,
130 and O_a horizons) were collected from each profile according to diagnostic horizons. The average

131 thickness of the organic soil horizon (O horizon) was ~98 cm. The O_i and O_e combined were ~38
132 cm in thickness, and the O_a horizon was ~60 cm. THg in the O_i , O_e , and O_a horizons of the forest
133 floor were based on two replicate soil cores from each of the five litter decomposition plots in
134 each forest stand. After freeze-dried, the samples were preserved in acid-cleaned polypropylene
135 containers at room temperature until further analysis. Litter and soil collections were done
136 monthly from March 2012 to February 2013.

137 **2.2.4 Hg volatilization from the forest field**

138 A dynamic flux chamber (DFC) in series with Tekran 1110 synchronized dual-port sampling unit
139 and Tekran automated Hg analyzer (2537X) were used to measure the emission rates of Hg^0 (Fu et
140 al., 2010). The special DFC method was described in detail at Ma et al. (2013). Hg emission
141 fluxes were calculated by the equation below (Ma et al., 2013):

$$142 \quad F = (C_{out} - C_{in}) \times Q / A$$

143 Where F is the flux ($ng\ m^2\ h^{-1}$); C_{out} and C_{in} are Hg^0 levels at the outlet and inlet of the Hg
144 analyzer ($ng\ m^3$); Q is the flushing flow rate through the chamber ($m^3\ h^{-1}$); and A is the surface
145 area of the soil exposed in the chamber (m^2).

146 Hg emission fluxes across the air/soil interface were monitored seasonally during eight intensive
147 field campaigns from spring 2012 to winter 2013 (Spring: March 4th-16th, May 8th -15th, 2012;
148 Summer: July 5th -12th, August 15th -22rd, 2012; Autumn: September 15th -22rd, October 20th -27th,
149 2012; Winter: December 24th -31st, 2012; February 6th -13th, 2013). Hg emission flux were
150 monitored at three sampling sites in the evergreen broadleaved forest of Mt. Simian. Hg emission
151 fluxes were measured continuously for 7 days for each sampling. Quality assurance was
152 conducted by manually injected Hg to the ambient air and soil vapor of the Tekran analyzer before
153 and after data collection. At the beginning and end of each measurement date, the Hg fluxes over a
154 clean TeflonTM sheet in the field was measured and regarded as the chamber blanks. The
155 chamber blanks in our research ranged from 0.48 to 0.64 $ng\ m^{-2}\ h^{-1}$, with an average of 0.54 ±
156 0.07 $ng\ m^{-2}\ h^{-1}$ (n=12). No blank value was needed to be subtracted from the flux due to no
157 significant difference found.

158 **2.3 Sample analysis and quality control**

159 For THg and MeHg in water samples, the special method was described at Ma et al. (2015).
160 Detailed introduction of the measurement of THg and MeHg in soil and litter samples can also be
161 found at Ma et al (2015). The detection limits of THg and MeHg in this research were 0.02 $ng\ L^{-1}$
162 and 0.01 $ng\ L^{-1}$ respectively. The dissolved total mercury (DHg), dissolved methylmercury
163 (DMeHg), particulate Hg (PHg) and particulate MeHg (PMeHg) were analyzed following the
164 EPA Method 1631 (US EPA, 1999). The method blank was lower than detection limits in all cases.
165 And the equipment blanks for THg and MeHg were 0.04 $ng\ L^{-1}$ and 0.02 $ng\ L^{-1}$, respectively. The
166 detection limits of Tekran 2537X was 0.1 $ng\ L^{-1}$ for GEM. The average relative standard deviation
167 for the duplicate analyses of THg and MeHg were 5.2% and 5.4%, respectively. Matrix spikes
168 recoveries for THg and MeHg were both within acceptable range, 89% to 115% for THg, and 91%
169 to 117% for MeHg. Precision was determined by relative standard deviations. For duplicate
170 samples, the precision were 5% for THg in water samples, 9% for MeHg in water samples, 8% for
171 THg in soil samples, and 4.1% for THg in leaf tissues.

172 **3. Results and discussion**

173 **3.1 Hg concentrations and deposition fluxes in throughfall and litterfall**

174 THg concentrations in the throughfall ranged from 3.2 to 62.5 $ng\ L^{-1}$ for the individual samples,

175 and the average level of throughfall was $24.1 \pm 7.9 \text{ ng L}^{-1}$. Canopy density did have an effect on
176 THg and MeHg concentrations (the forest cover is more than 90% and the canopy density is 0.9).
177 THg concentrations measured in the throughfall of the subtropical evergreen broad-leaved forest
178 ($24.1 \pm 7.9 \text{ ng L}^{-1}$) were significantly higher than those measured in the open field ($10.9 \pm 3.1 \text{ ng}$
179 L^{-1}). Similar to THg concentrations, MeHg concentrations in the throughfall were nearly 2.5 times
180 higher than that in precipitation ($p=0.004$, $n=49$).

181

182 THg concentrations in the throughfall were consistently at their highest in the cold season (Fig.1),
183 which was probably due to the lower rainfall but elevated atmospheric Hg in this season. In the
184 subtropical region of China, the monsoon-driven climate of northwest China doesn't bring much
185 precipitation in cold season. At the same time, atmospheric stability is high during the cold period,
186 and pollutants like atmospheric Hg do not spread easily, which contributes to the higher
187 scavenging ability of Hg in the atmosphere. While the warm season (from April to September) is
188 influenced by the southeast monsoon, and the rainfall increases greatly, which leads to lower
189 concentration of Hg (Fig.1). The study station has obscure seasons and clear rainy and dry seasons.
190 The deposition fluxes of THg through throughfall also showed the seasonal variation
191 characteristics, with higher fluxes appearing in wet-season (June to August). The deposition fluxes
192 of THg through throughfall in summer at Mt. Simian accounted more than 40% of total annual Hg
193 deposition. However, it is still in September and October that a higher throughfall flux is observed.
194 This may be because that the rainfall in the two months is mainly effected by Indian Monsoon,
195 contributing to a higher rainfall (Fu et al., 2008a) comparing with other months. The minimum
196 values for THg deposition occurred in the cold season.

197

198 During the surveillance, THg in the throughfall was evaluated to be $32.2 \mu\text{g m}^{-2} \text{ yr}^{-1}$. The
199 deposition fluxes of THg through throughfall in Mt. Simian were lower than those investigated in
200 the southwestern cities of China, such as Guizhou and Chongqing (Precipitation: $8.4\text{--}62.1 \mu\text{g m}^{-2}$
201 yr^{-1} , throughfall: $15.6\text{--}292.1 \mu\text{g m}^{-2} \text{ yr}^{-1}$, Guo et al., 2008; Feng et al., 2009a,b; Wang et al., 2007).
202 However, the deposition fluxes of THg through throughfall in Mt. Simian were approximately
203 2–10 times higher than those reported in remote areas of North America and Europe (Precipitation:
204 $3.1\text{--}10.0 \mu\text{g m}^{-2} \text{ yr}^{-1}$, throughfall: $6.7\text{--}23.0 \mu\text{g m}^{-2} \text{ yr}^{-1}$, St. Louis et al., 2001; Keeler et al., 2005).
205 Obviously, the THg fluxes at Mt. Simian were higher than other sites abroad. The reason perhaps
206 was that Mt. Simian had considerably more dense forest canopies. As one of the National Natural
207 Reserves of China, it has preserved the best subtropical evergreen broad-leaved forest of China.
208 The forest cover in the reserves reaches over 90%. The increased THg concentrations in
209 throughfall mainly resulted from the dry deposition of Hg on the vegetation, followed by the
210 washout of throughfall. Another possible reason for the elevated deposition fluxes, which may be
211 the most important one, probably related with the increased atmospheric Hg concentrations in the
212 past 30 years due to China's fast economic development. This area, especially Chongqing city, has
213 a large demand for energy consumption, and about 70% of which is from coal combustion. The
214 annual mean gaseous elemental Hg (GEM) concentration in the middle of Chongqing city
215 ($9.6\text{--}31.9 \text{ ng m}^{-3}$, Wang et al., 2006), more than 200 km away from the study site, tripled
216 comparing with global background level (Lindberg et al., 2002a, b), which corresponded to the
217 high annual deposition flux of Hg in the study area. It is also reported that the GEM concentration
218 in the study area is as high as $3.8 \pm 1.5 \text{ ng m}^{-3}$ (Ma et al., 2015), even if it is situated in a natural

219 subtropical forest reserve. The MeHg flux was $0.45 \mu\text{g m}^{-2} \text{yr}^{-1}$, which was higher than those
220 measured in other areas. While MeHg/THg in the throughfall samples was 1.3 %, which was a
221 relatively high value compared with other studies (0.4%-0.8%, Lee et al., 2000; Demers et al.,
222 2007; Choi et al., 2008; Fu et al., 2008a; Guo et al., 2008; Larssen et al., 2008). Here, the higher
223 ratio of MeHg to THg in throughfall samples may suggest that the contribution of MeHg from
224 throughfall cannot be ignored and should be taken care of in future studies. After all,
225 accumulation of MeHg in the soil might have caused serious risks in the functioning of natural
226 downstream ecosystems.

227

228 The deposition fluxes of THg through litterfall are shown in Table 1. The average concentrations
229 of THg and MeHg in leaf litter were $106.7 \pm 8.3 \text{ ng g}^{-1}$ (SE = 2.6, N=60) and $0.8 \pm 0.4 \text{ ng g}^{-1}$ (SE =
230 0.2, N=60), respectively. The deposition flux of THg through litterfall was estimated to be $42.9 \mu\text{g}$
231 $\text{m}^{-2} \text{yr}^{-1}$ in the measurement field, which was remarkably higher than the input flux through
232 throughfall. It is also considerably higher than litterfall fluxes reported from other regions (St.
233 Louis et al., 2001; Demers et al., 2007). GEM can be absorbed by stomata and detained in the leaf
234 tissue (Ericksen et al., 2003; Fu et al., 2008a, b). Therefore, we believed that the elevated litterfall
235 input fluxes directly related to the increased GEM concentrations, even in remote areas.

236 **3.2 Mercury emission from soils under the canopy**

237 The emission characteristics and air-surface exchange of GEM from the subtropical forest field
238 have been investigated during eight intensive field campaigns from 2012 to 2013. At the forest
239 field, GEM released from soils had the characteristic of obvious diurnal and seasonal variations.
240 Day and night GEM fluxes were statistically different (t-test, $p < 0.001$), with nighttime emissions
241 considerably lower than that in daytime in all seasons (Fig.2). Average fluxes of Hg in spring,
242 summer, autumn and winter were $12.2 \pm 5.1 \text{ ng m}^{-2} \text{h}^{-1}$, $14.2 \pm 4.7 \text{ ng m}^{-2} \text{h}^{-1}$, $9.9 \pm 2.5 \text{ ng m}^{-2} \text{h}^{-1}$,
243 and $3.1 \pm 1.1 \text{ ng m}^{-2} \text{h}^{-1}$, respectively. It can be seen that the highest value occurred in summer,
244 followed by spring and fall, while the lowest value was observed in winter. The average fluxes of
245 Hg in spring ($12.2 \pm 5.1 \text{ ng m}^{-2} \text{h}^{-1}$) were slightly lower than that in summer ($14.2 \pm 4.7 \text{ ng m}^{-2}$
246 h^{-1}), which was different from other studies (Larssen et al., 2008; Fu et al., 2010). It appeared that
247 warm temperature with low canopy density in spring at the mid subtropical forest were more
248 likely to release GEM. Perhaps the primary reason lies that the forest canopies are lushly and well
249 spaced in spring, and thus the forest can receive more sunlight. Therefore, the reduction rate of
250 Hg^{2+} by photochemical, thermal and biogenic processes probably increased.

251 This research indicated that Hg fluxes of forest field were far lower than those observed from
252 contaminated areas such as heavily air-polluted areas in eastern Guizhou ($33\text{--}3638 \text{ ng m}^{-2} \text{h}^{-1}$)
253 (Wang et al., 2007), some cities in southwest China ($15.0\text{--}44.4 \text{ ng m}^{-2} \text{h}^{-1}$) (Qiu et al., 2006), dry
254 landfills ($46.5\text{--}22.8 \text{ ng m}^{-2} \text{h}^{-1}$) (Zhu et al., 2010) and wetlands ($20\text{--}500 \text{ ng m}^{-2} \text{h}^{-1}$) (Lindberg et
255 al., 2002b). But the emission of GEM elevated in comparison with those reported from other
256 places ($-5.4\text{--}4.2 \text{ ng m}^3$, Lindberg et al., 2002a, b; $1.7\text{--}8.4 \text{ ng m}^3$, Travnikov, 2005). At Mt. Simian,
257 the estimated net GEM fluxes were released from soils during the warm season and slightly
258 volatilized during the cold season. Hg deposition was only observed in several nights of the cold
259 season during the study period. Hg released from the snow/air interface was extremely low
260 comparing with the soil/air interface. It was supposed that the Hg^0 flux was zero from
261 snow-covered surface (Huang et al., 2012). At most subtropical areas, especially mid-subtropical
262 forests, however, there were short winter seasons with unstable snow cover, and the snow cover

263 season only tended to occur in January. So we assumed that there still existed Hg⁰ emission in
264 December and February in winter. Therefore, the annual total net Hg emission flux was 18.6 mg
265 m⁻² yr⁻¹.

266 **3.3 Hg concentrations and out-flux in stream water**

267 Annual volume-weighted concentrations of THg and MeHg were measured at the outlet stream of
268 the forest field of Mt. Simian. The mean concentrations of THg and MeHg in the outflow stream
269 were 3.9 ±2.0 and 0.2±0.08 ng L⁻¹, respectively. THg and MeHg concentrations in stream water
270 draining the upland in our research were slightly higher than those reported in literature (Fu et al.,
271 2008a, b; Larssen et al., 2008). THg concentrations in runoff/stream water in rainy seasons
272 (4.6±2.0ng L⁻¹) were significantly higher than those in dry seasons (3.3±1.8 ng L⁻¹), which can
273 probably be attributed to the soil erosion and runoff (Ma et al., 2015). It is known that if a remote
274 forest field does not have other obvious Hg pollution sources, Hg concentrations in the
275 runoff/stream water can represent risks from a solitary watershed. Numerous studies showed that
276 the catchments of remote forest were regarded as filters between atmosphere and hydrosphere
277 (Lee et al., 2000; Larssen et al., 2008; Ericksen et al., 2003). The fate of Hg stored in the forest
278 soils can be divided into three parts. One part of them transfers through food webs, threatening the
279 balance of forest ecosystems; the second part of them is released into the atmosphere again; the
280 third part of them probably transfers with the runoff/stream, becoming one of the Hg sources of
281 downstream aquatic ecosystem. Therefore, to a certain extent, the role of forested catchments as
282 Hg filters can be characterized by Hg output (runoff/stream) from the forest field.

283 This study showed that, even though Hg deposition fluxes in throughfall was high, THg
284 concentration in stream/runoff was lower than that in contaminated sites under the same
285 geological background. This indicated that subtropical forest field had the filtering effect of Hg in
286 precipitation and throughfall. On the other hand, the lower concentration in stream/runoff
287 indicated that the study area did not suffer from severe anthropogenic Hg pollution. Steam output
288 of THg was calculated by multiplying the average THg concentration in stream water (3.9 ±2.03
289 ng L⁻¹) by the water discharge rate in the forest field of the study site (annual water discharge:
290 1.86×10⁸ m³, from hydrological departments of Jiangjin district). The export flux of THg via
291 runoff/stream was 0.73 kg yr⁻¹. The subtropical forest field in the study area is 100.1 km². So the
292 export flux of THg through stream water was 7.23 μg m⁻² yr⁻¹, which tripled the values reported
293 in the catchments of Sweden (1.6–1.8 μg m⁻² yr⁻¹, Lee et al., 2000; 2.4 μg m⁻² yr⁻¹, Larssen et al.,
294 2008). Our results indicated that the output fluxes of MeHg via stream water were 0.08 μg m⁻²
295 yr⁻¹, which was similar to or slightly larger than other results (0.03–0.07 μg m⁻² yr⁻¹, Lee et al.,
296 2000; 0.05 μg m⁻² yr⁻¹, Schwesig and Matzner, 2001). As we mentioned above that Mt. Simian
297 was one of the most complete forest and until recent decades was one of Asia's
298 least populated and most inaccessible areas. Average Hg concentration in the soil detected in
299 previous research was 0.28 mg kg⁻¹ (Ma et al., 2013), which indicated that it was not an obvious
300 geological Hg hotspot. Therefore, the elevated Hg fluxes in stream water were probably attributed
301 to the great atmospheric Hg depositions. At the same time, our preliminary research results also
302 illustrated that forest runoff and soil erosion could increase Hg output from subtropical forest
303 catchments (Ma et al., 2013). But the total output fluxes of THg and MeHg were far lower than
304 the input fluxes via wet deposition (32.2 μg m⁻² yr⁻¹ for THg and 0.5 μg m⁻² yr⁻¹ for MeHg). This
305 study showed that the subtropical forest was able to exert purification effect of filtration, even
306 under the condition of elevated deposition of Hg.

307 3.4. Dynamics and transport of Hg based on forest field

308 THg content in the forest field (forest floor and soil profiles) of Mt. Simian was shown in Table 2.
309 The THg stocked in the forest soil was approximately $20192 \mu\text{g m}^{-2}$ (average soil depth is 98 cm),
310 while that in the organic floor was $5148 \mu\text{g m}^{-2}$ (average litter depth is 19 cm). THg content in soil
311 profile were three times more than the organic horizon in the subtropical forest field. The active
312 pool (the upper 22 cm, O_i) of THg represented 41 % of the total storage of the study area. In the
313 soil profile, THg content in the organic horizon (O_i) is obviously higher than those in the other
314 horizons. At the same time, the organic matter is well decomposed under warm and rainy
315 subtropical climate, which has high affinity to Hg in soil.
316 Due to the good adsorption and reduction of organic matter, the organically bound contents of Hg
317 could be released into the environment again during the decomposition of organic matter.

318 The ultimate fate of Hg in the terrestrial ecosystem may depend upon its delivery and
319 incorporation into the forest floor. And the average Hg fluxes were also estimated. Input of THg to
320 the forest field of Mt. Simian included net throughfall and litterfall depositions (St. Louis et al.,
321 2001; Fu et al., 2010). Annual throughfall and litterfall deposition fluxes of THg in Mt. Simian
322 were 32.2 and $42.9 \text{ mg m}^{-2} \text{ y}^{-1}$, respectively (Fig.3). Litterfall deposition inputs were estimated to
323 134% of the throughfall deposition at the forest field. In the study forest field, the predominant
324 pathway of Hg fluxes to the forest floor was via litterfall (57.1%). A majority of atmospherically
325 deposited THg was released through Hg^0 at a rate of $18.6 \mu\text{g m}^{-2} \text{ y}^{-1}$. Steam outflow of THg from
326 the wetland was $7.2 \mu\text{g m}^{-2} \text{ yr}^{-1}$. The ratio between output and input of THg was 0.34 at the
327 subtropical forest field of Mt. Simian, which was significantly higher than others (0.02-0.04, Lee
328 et al., 2000; 0.16, Larssen et al., 2008; 0.30, Fu et al., 2010). The apparently higher ratio between
329 the output/input fluxes of THg may represent an important ecological risk.

330 The THg stored in the forest field was 982 times larger than the annual THg output by
331 stream/runoff outflow and soil volatilization, and 338 times larger than the input estimated from
332 wet and dry depositions (Fig.3). The estimates of the deposition flux of THg in this study were
333 much higher than values reported from the northeastern American ($3.8\text{--}12.6 \mu\text{g m}^{-2} \text{ yr}^{-1}$; Driscoll
334 et al., 2007) and Norway ($7 \mu\text{g m}^2 \text{ yr}^{-1}$; Larssen et al., 2008), probably indicating a significant
335 impact of heavy regional Hg emissions from industry and urban on local Hg deposition. The
336 reason perhaps was that highly soluble Hg^{2+} was easily stripped from the atmosphere and
337 deposited locally. Higher wet deposition can illustrate the remarkable influence of local Hg
338 emissions on Hg accumulation in the regional forest field. The THg flux through litterfall was 1.5
339 times larger than that through throughfall due to greater input of litter mass and higher Hg
340 concentrations in the litter. Annual exports of THg in stream water of the study area ($3.2\text{--}9.5 \mu\text{g}$
341 $\text{m}^{-2}\text{yr}^{-1}$) were not accorded with those reported from northern forest catchments ($1.0\text{--}3.4 \mu\text{g m}^{-2}$
342 yr^{-1} ; St. Louis et al., 2001; Grigal et al., 2000). An amount of the atmospherically deposited THg
343 was lost via emissions at a rate of $18.6 \mu\text{g m}^{-2} \text{ yr}^{-1}$. Compared with stream outflow, the evasion of
344 Hg from forest soil played a more essential role in THg outputs.

345 Compared the ratios of output to input flux with other places (Larssen et al., 2008; Fu et al., 2010),
346 the higher ratio may be greatly affected by the elevated deposition. Therefore, regional emission
347 of Hg may have stronger influence on forest ecosystems, in which the deposition of THg through
348 litterfall and throughfall, being affected more by local and regional changes of Hg emissions and
349 cycling, were the main paths for Hg entering into soil surface (Demers et al., 2007). However, in
350 this study, the outflow of Hg via runoff output and the soil-air interface accounted for a small

351 fraction of Hg budget in the study area. And the accumulation pattern of Hg in forest floor and soil
352 profiles was seasonal. As we mentioned above that Mt. Simian was one of the most typical
353 subtropical forest systems and the least accessed area, average Hg concentrations in all soil
354 surfaces of this area were below 0.30 mg kg^{-1} (Fu et al., 2010; Ma et al., 2013). Therefore, the
355 accumulation of Hg in soil would be enhanced with time. At the same time, the ultimate fate of
356 deposited Hg depends upon the biogeochemical processes that have not been well quantified
357 within the ecosystem. Hg dynamics during litter decomposition, for instance, need to be
358 considered as a whole so that we can better understand controls on long-term accumulation of Hg
359 in the forest ecosystem and its delayed release to surface water.

360 **4. Conclusions**

361 In this study, the mass balance and transport of Hg in southwestern China were first measured at a
362 subtropical forest, Chongqing, China. Results revealed that litterfall deposition inputs were the
363 predominant pathway ($42.9 \text{ mg m}^{-2} \text{ y}^{-1}$, account for 57.1%) of Hg flux to the forest floor. Annual
364 deposition fluxes of Hg through throughfall were $32.2 \text{ m}^{-2} \text{ y}^{-1}$, accounting for 42.9% of the Hg
365 inputs. Researchers should pay more attention to the higher ratio of MeHg to THg in the
366 throughfall deposition when they model the biogeochemical cycling in a typical local forest
367 watershed. For the output process, the exchange of Hg ($18.6 \text{ } \mu\text{g m}^{-2} \text{ y}^{-1}$) across the forest field-air
368 interface was an essential part of the biogeochemical cycle of Hg. The runoff/steam outflow of
369 THg from the wetland was $7.2 \text{ mg m}^{-2} \text{ yr}^{-1}$, which was lower than that in contaminated sites under
370 the same geological background. Therefore, we may conclude that: 1) the study area does not
371 suffer from severe anthropogenic Hg pollution; 2) the forested field has the filtering effect of Hg
372 in precipitation and throughfall, even in the elevated atmospheric Hg area.

373 The forest field (forest floor and soil profiles) plays an important role in the cycling of THg and
374 MeHg. In reality, it is just another problem created by the accumulation of Hg,
375 which would be a potential risk affecting the output of Hg in the long term. Terrestrial ecosystems
376 that have accumulated more Hg may ultimately emit them to the wetlands and surface water,
377 finally affecting the entire aquatic ecosystems. Therefore, it is a signal that we should not ignore.
378 In this case, however, any changes in the forest floor like deforestation or forestland degradation
379 may strongly affect Hg budget of the region.

380 **Data availability**

381 Data in this research is available from the email of Professor D.Y. Wang,
382 dywang@swu.edu.cn.

383 **Author contribution**

384 Ma M, Sun T, Du H and Zhao Z collected the litterfall, throughfall, stream water and forest soil
385 samples. Wang Y measured the concentrations of THg and MeHg from all samples. Sun T made
386 the analysis of Hg volatilization from forest field. Ma M wrote the main manuscript text and drew
387 all the figures, with contributions from all co-authors. Wang D, Wei S and Ma M designed the
388 research. All authors reviewed the manuscript.

389 **Acknowledgements**

390 We are also grateful to Vincent Grondin (University of Qu bec at Montreal) for his language
391 modification on the early draft of the manuscript. This study was supported by the Natural Science
392 Foundation of China (41573105), the National Basic Research Program of China (973 Program,
393 2013CB430003), and the Fundamental Research Funds for the Central Universities
394 (XDJK2013B044).

396 **References**

- 397 Choi, H. D., Sharac, T. J., and Holsen, T. M.: Mercury deposition in the Adirondacks: A
398 comparison between precipitation and throughfall, *Atmos. Environ.*, 42(8), 1818–1827,
399 doi:10.1016/j.atmosenv.2007.11.036, 2008.
- 400 Demers, J. D., Driscoll, C. T., Fahey, T. J., and Yavitti, J. B.: Mercury cycling in litter and soil in
401 different forest types in the Adirondack region, New York, USA, *Ecol. Appl.*, 17(5), 1341–1351,
402 doi:10.1890/06-1697.1, 2007.
- 403 Driscoll, C. T., Han Y. J., Chen, C.Y., Evers, D. C., Lambert, K. F., Holsen, T. M., Kamman, N.
404 C., and Munson, R.K.: Mercury contamination in forest and freshwater ecosystems in the
405 northeastern United States. *BioScience*, 57, 17–28, doi:10.1641/B570106, 2007.
- 406 Ericksen, J. A., Gustin, M. S., Schorran, D. E., Johnson, D. W., Lindberg, S. E., and Coleman, J.
407 S.: Accumulation of atmospheric mercury in forest foliage, *Atmos. Environ.*, 37(12), 1613–1622,
408 doi:10.1016/S1352-2310(03)00008-6, 2003.
- 409 Feng, X., and Qiu, G.: Mercury pollution in Guizhou, Southwestern China– an overview, *Sci.*
410 *Total Environ.*, 400, 227–237, doi:10.1016/j.scitotenv.2008.05.040, 2008.
- 411 Feng, X., Jiang, H., Qiu, G., Yan, H., Li, G., and Li, Z.: Mercury mass balance study in
412 Wujiangdu and Dongfeng reservoirs, Guizhou, China, *Environ. Pollut.*, 157, 2594–2603,
413 doi:10.1016/j.envpol.2009.05.024, 2009a.
- 414 Feng, X., Jiang, H., Qiu, G., Yan, H., Li, G., and Li, Z.: Geochemical processes of mercury in
415 Wujiangdu and Dongfeng reservoirs, Guizhou, China, *Environ. Pollut.*, 157, 2970–2984,
416 doi:10.1016/j.envpol.2009.06.002, 2009b.
- 417 Fu, X., Feng, X., Dong, Z., Yin, R., Wang, J., Yang, Z., and Zhang, H.: Atmospheric gaseous
418 elemental mercury (GEM) concentrations and mercury depositions at a high-altitude mountain
419 peak in south China, *Atmos. Chem. Phys.*, 10, 2425–2437, doi:10.5194/acp-10-2425-2010, 2008a.
- 420 Fu, X., Feng, X., Zhu, W., Wang, S., and Lu, J.: Total gaseous mercury concentrations in ambient
421 air in the eastern slope of Mt. Gongga, South-Eastern fringe of the Tibetan plateau, China, *Atmos.*
422 *Environ.*, 42, 70–979, doi:10.1016/j.atmosenv.2007.10.018, 2008b.
- 423 Fu, X., Feng, X., Wang, S., Rothenberg, S., Shang, L., Li, Z., and Qiu, G.: Temporal and spatial
424 distributions of total gaseous mercury concentrations in ambient air in a mountainous area in
425 southwestern China: Implications for industrial and domestic mercury emissions in remote areas
426 in China, *Sci. Total Environ.*, 407, 2306–2314, doi:10.1016/j.scitotenv.2008.11.053, 2009.
- 427 Fu, X., Feng, X., Zhu, W., Rothenberg, S., Yao, H., and Zhang, H.: Elevated atmospheric
428 deposition and dynamics of mercury in a remote upland forest of Southwestern China, *Environ.*
429 *Pollut.*, 158, 2324–2333, doi:10.1016/j.envpol.2010.01.032, 2010.
- 430 Grigal, J. A., Kolka, R. K., Fleck, J. A., and Nater, E. A.: Mercury budget of an upland-peatland
431 watershed, *Biogeochemistry*, 50(1), 95–109, doi: 10.1023/A:1006322705566, 2000.
- 432 Guo, Y., Feng, X., Li, Z., He, T., Yan, H., Meng, B., Zhang, J., and Qiu, G.: Distribution and wet
433 deposition fluxes of total and methyl mercury in Wujiang reservoir Basin, Guizhou, China, *Atmos.*
434 *Environ.*, 42, 7096–7103, doi:10.1016/j.atmosenv.2008.06.006, 2008.
- 435 Huang, J., Kang, S., Zhang, Q., Jenkins, M., Guo, J., Zhang, G., and Wang, K.: Spatial distribution
436 and magnification processes of mercury in snow from high-elevation glaciers in the Tibetan
437 Plateau, *Atmos. Environ.*, 46 (1), 140–146, doi:10.1016/j.atmosenv.2011.10.008, 2012.
- 438 Keeler, G. J., Gratz, L. E., and Al-wali, K.: Long-term atmospheric mercury wet deposition at

439 Underhill, Vermont, *Ecotoxicology*, 14(1–2), 71–83, doi:10.1007/s10646-004-6260-3, 2005.

440 Larssen, T., De Wit, H. A., Wiker, M., and Halse, K.: Mercury budget of a small forested boreal
441 catchment in southeast Norway, *Sci. Total Environ.*, 404(2–3), 290–296,
442 doi:10.1016/j.scitotenv.2008.03.013, 2008.

443 Lee, Y. H., Bishop, K. H., and Munthe, J.: Do concepts about catchment cycling of
444 methylmercury and mercury in boreal catchments stand the test of time? Six years of atmospheric
445 inputs and runoff export at Svartberget, northern Sweden, *Sci. Total Environ.*, 260, 11–20,
446 doi:10.1016/S0048-9697(00)00538-6, 2000.

447 Lindberg, S. E., Zhang, H., Vette, A. F., Gustin, M. S., Barnett, M. O., and Kuiken, T.: Dynamic
448 flux chamber measurement of gaseous mercury emission fluxes over soils, Part 2: effect of
449 flushing flow rate and verification of a two-resistance exchange interface simulation model.
450 *Atmos. Environ.*, 36, 847–859, doi:10.1016/S1352-2310(01)00502-7, 2002a.

451 Lindberg, S. E., Dong, W., and Meyers, T.: Transpiration of gaseous elemental mercury through
452 vegetation in a subtropical wetland in Florida. *Atmos. Environ.*, 36, 5207–5219, doi:
453 10.1016/S1352-2310(02)00586-1, 2002b.

454 Lv, W., Zhang, H., Wang, W., Du, S., Wu, Y., He, P., and Xiao, L.: Characteristics of soil
455 aggregates in different forestlands in Simian mountains, Chongqing, *J. Soil Water Conserv.*,
456 24(4):193-197, doi:10.13870/j.cnki.stbcxb.2010.04.048, 2014.

457 Ma, M., Wang, D., Du, H., Sun, R., Zhao, Z., and Wei, S.: Gaseous mercury emissions from
458 subtropical forested and open field soils in a national nature reserve, southwest China, *Atmos.*
459 *Environ.*, 64, 116–123, doi:10.1016/j.atmosenv.2012.09.038, 2013.

460 Ma, M., Wang, D., Sun, R., Shen, Y., and Huang, L.: Atmospheric mercury deposition and its
461 contribution of the regional atmospheric transport to mercury pollution at a national forest nature
462 reserve, southwest China, *Environ. Sci. Pollut. Res.*, online, doi: 10.1007/s11356-015-5152-9,
463 2015.

464 Qiu, G., Feng, X., Wang, S., and Shang, L.: Environmental contamination of mercury from
465 Hg-mining areas in Wuchuan, northeastern Guizhou, China, *Environ. Pollut.*, 142 (3), 549–558,
466 doi:10.1016/j.envpol.2005.10.015, 2006.

467 Schwesig, D., and Matzner, E.: Dynamics of mercury and methylmercury in forest floor and
468 runoff of a forested watershed in Central Europe, *Biogeochemistry*, 53(2), 181–200, doi:
469 10.1023/A:1010600600099, 2001.

470 Sigler, J. M., Mao, H., and Talbot, R.: Gaseous elemental and reactive mercury in Southern New
471 Hampshire, *Atmos. Chem. Phys.*, 9, 1929–1942, doi:10.5194/acp-9-1929-2009, 2009.

472 St. Louis, V. L., Rudd, W. M., Kelly, C. A., Hall, B. D., Rolfhus, K. R., Scott, K. J., Lindberg, S.
473 E., and Dong, W.: Importance of the forest canopy to flux of methylmercury and total mercury to
474 boreal ecosystems, *Environ. Sci. Technol.*, 35, 3089–3098, doi: 10.1021/es001924p, 2001.

475 Stamenkovic, J., and Gustin, M. S.: Nonstomatal versus Stomatal uptake of atmospheric mercury,
476 *Environ. Sci. Technol.*, 43, 1367–1372, doi: 10.1021/es801583a, 2009.

477 Travnikov, O.: Contribution of the intercontinental atmospheric transport to mercury pollution in
478 the Northern Hemisphere, *Atmos. Environ.*, 39, 7541–7548, doi:10.1016/j.atmosenv.2005.07.066,
479 2005.

480 US EPA: Method 1631: Revision B, Mercury in water by Oxidation, Purge and Trap, and Cold
481 Vapor atomic Fluorescence Spectrometry, United States Environmental Protection Agency, 1–33,
482 1999.

483

484 Wang, D., He, L., Shi, X., Wei, S., and Feng, X.: Release flux of mercury from different
 485 environmental surfaces in Chongqing, China, *Chemosphere*, 64(11), 1845-1854,
 486 doi:10.1016/j.chemosphere.2006.01.054, 2006.

487 Wang, S., Feng, X., Qiu, G., Fu, X., and Wei, Z.: Characteristics of mercury exchange flux
 488 between soil and air in the heavily air-polluted area, eastern Guizhou, China, *Atmos. Environ.*,
 489 41(27), 5584–5594, doi:10.1016/j.atmosenv.2007.03.002, 2007.

490 Zhu, J., Wang, D., Liu, X., and Zhang, Y.: Mercury fluxes from air/surface interfaces in paddy
 491 field and dry land, *Appl. Geochemistry*, 26(2), 249–255, doi:10.1016/j.apgeochem.2010.11.025,
 492 2010.

493

494

Tables

495 Table 1 Mean values of THg and MeHg concentrations and deposition fluxes in throughfall and
 496 litterfall

	THg Concentration (ng L ⁻¹)			MeHg Concentration (ng L ⁻¹)		
	THg	DHg	PHg	MeHg	DMeHg	PMeHg
Precipitation	10.94±3.1	4.43±2.2	6.52±2.9	0.24±0.34	0.11±0.04	0.13±0.10
Throughfall	24.04 ±7.9	6.68 ±4.2	16.35±5.7	0.33 ±0.24	0.25 ±0.12	0.31 ±0.14
Litterfall	THg Concentration (ng g ⁻¹)			MeHg Concentration (ng g ⁻¹)		
	106.7±18.3			0.79±0.36		
Annual deposition flux	THg (µg m ⁻² yr ⁻¹)			MeHg (µg m ⁻² yr ⁻¹)		
Precipitation (1508mm)	15.45			0.36		
Throughfall (1336mm)	32.17			0.45		
Litterfall (402g m ⁻² yr ⁻¹)	42.89			0.32		

497

498

499

500

501

502

503

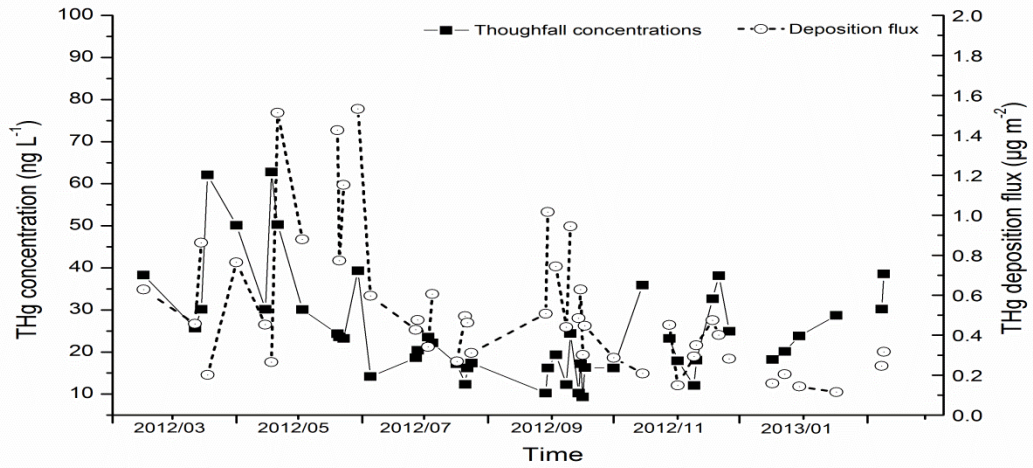
Table 2 The concentrations and contents of THg in forest floor and different soil layers

		THg (ng g ⁻¹)	Density (g cm ⁻³)	Thickness (m)	THg content(µg m ⁻²)	Total contents
	Initial leaf litter	46.30±14.2	0.28±6.2	0.06±0.02	774.8	
Forest floor	Half decomposition	51.22±9.4	0.49±18.1	0.08±0.03	2000.8	5148.7
	decomposition	57.88±10.3	0.82±9.9	0.05±0.02	2373.1	
	<i>O_i</i>	297.8±15.2	1.27±2.1	0.22±0.10	8320.5	
Soil profile	<i>O_e</i>	117.4±32.3	1.65±16.2	0.34±0.08	6586.1	20192.6
	<i>O_a</i>	68.4±13.6	1.84±20.7	0.42±0.06	5286.0	

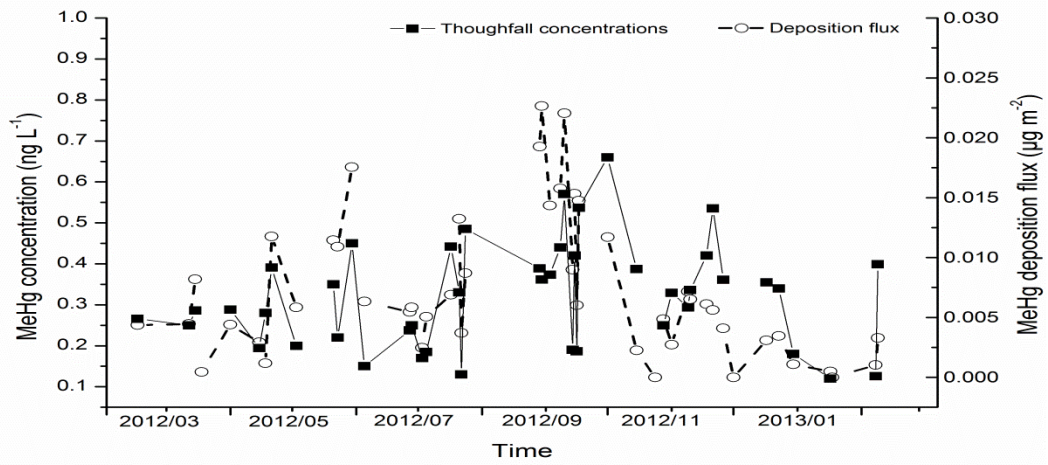
504

505

Figures



506

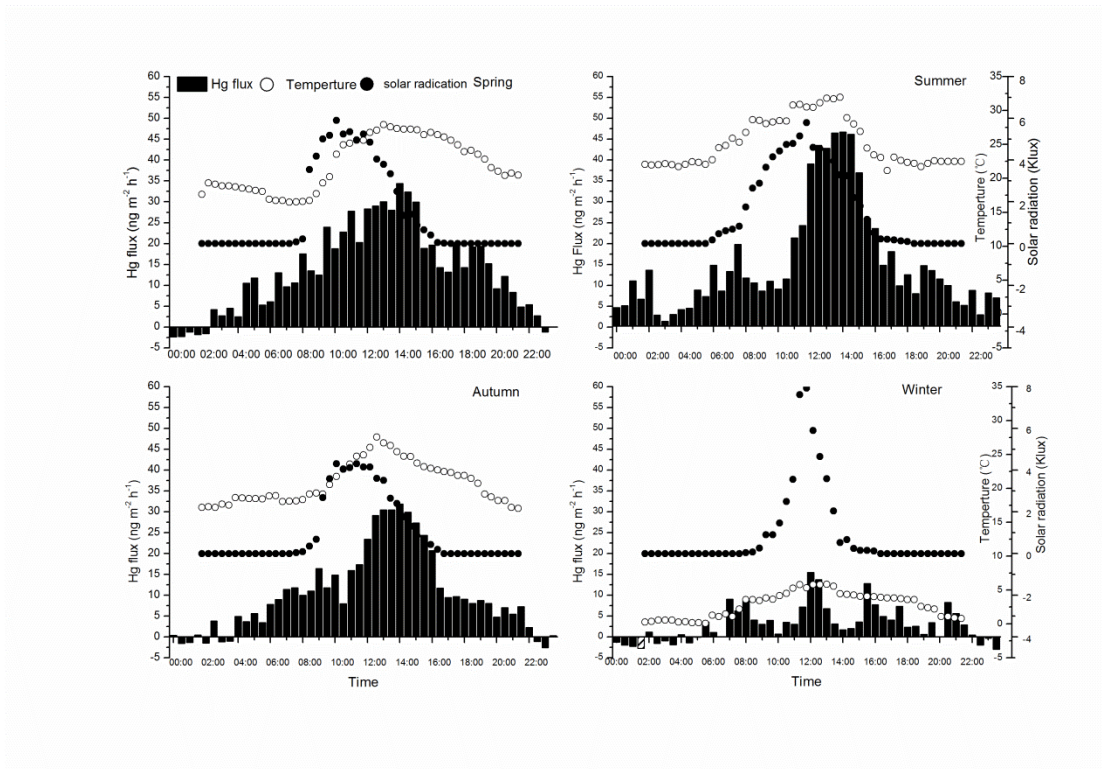


507

508

509

Fig. 1. Volume-weighted mean concentrations of THg and MeHg and deposition fluxes of throughfall in the evergreen broad-leaf forest from March 2012 to February 2013



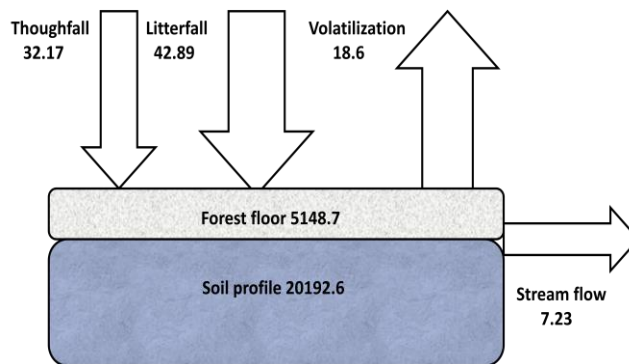
510

511 Fig. 2. Soil emission fluxes of Hg and air temperature in the evergreen broad-leaf forest field.
 512 Spring: March 4th-16th, May 8th-15th, 2012; Summer: July 5th-12th, August 15th-22rd, 2012;
 513 Autumn: September 15th-22rd, October 20th-27th, 2012; Winter: December 24th-31st, 2012;
 514 February 6th-13th, 2013.

515

516

517



518

519 Fig.3. Annual ecosystem Hg fluxes and pools in the evergreen broad-leaf forest field. Fluxes (μg
 520 $\text{m}^{-2} \text{yr}^{-1}$) were represented by arrows, while pools ($\mu\text{g} \text{m}^2$) by boxes.